

Strategies to mitigate aliasing of loading signals while estimating GPS frame parameters

Xavier Collilieux · Tonie van Dam · Jim Ray ·
David Coulot · Laurent Métivier · Zuheir Altamimi

Received: 17 January 2011 / Accepted: 17 May 2011 / Published online: 8 June 2011
© Springer-Verlag 2011

Abstract Although GNSS techniques are theoretically sensitive to the Earth center of mass, it is often preferable to remove intrinsic origin and scale information from the estimated station positions since they are known to be affected by systematic errors. This is usually done by estimating the parameters of a linearized similarity transformation which relates the quasi-instantaneous frames to a long-term frame such as the International Terrestrial Reference Frame (ITRF). It is well known that non-linear station motions can partially alias into these parameters. We discuss in this paper some procedures that may allow reducing these aliasing effects in the case of the GPS techniques. The options include the use of well-distributed sub-networks for the frame transformation estimation, the use of site loading corrections, a modification of the stochastic model by downweighting heights, or the joint estimation of the low degrees of the deformation field. We confirm that the standard approach consisting of estimating the transformation over the whole network is particularly harmful for the loading signals if the network is not well distributed. Downweighting the height component, using a uniform sub-network, or estimating the deformation

field perform similarly in drastically reducing the amplitude of the aliasing effect. The application of these methods to reprocessed GPS terrestrial frames permits an assessment of the level of agreement between GPS and our loading model, which is found to be about 1.5 mm WRMS in height and 0.8 mm WRMS in the horizontal at the annual frequency. Aliased loading signals are not the main source of discrepancies between loading displacement models and GPS position time series.

Keywords Loading effects · Terrestrial Reference Frame · GNSS · GPS · Geocenter motion

1 Introduction

Global Navigation Satellite System (GNSS) techniques, especially the Global Positioning System (GPS), are used to accurately monitor ground deformations on timescales from sub-second to decadal. The most accurate processing strategies consist of processing GNSS data received at a wide set of global stations simultaneously using the most current and consistent models. All the phenomena that affect the GNSS observables need to be parameterized or modeled, especially if their time scales of variation are shorter than the sampling rate of the estimated parameters. This is the case for solid Earth tides, pole tides, and ocean tidal loading effects which are well modeled (McCarthy and Petit 2004). Non-tidal loading effects, which include the effect of the atmosphere, ocean circulation, and hydrological loading are still under investigation. Correlations have been noted with space geodetic results, namely from GPS (van Dam et al. 1994, 2001), Very Long Baseline Interferometry (VLBI) (van Dam and Herring 1994; Petrov and Boy 2004), Satellite Laser Ranging (SLR) and Doppler Orbitography Integrated on Satellites (DORIS)

X. Collilieux (✉) · D. Coulot · L. Métivier · Z. Altamimi
IGN/LAREG et GRGS, 6-8 av. Blaise Pascal,
77455 Marne La Vallée Cedex 2, France
e-mail: xavier.collilieux@ign.fr

T. van Dam
University of Luxembourg, 162a, avenue de la Faïencerie,
1511 Luxembourg, Luxembourg

J. Ray
NOAA National Geodetic Survey, 1315 East-West Hwy,
Silver Spring, MD 20910, USA

L. Métivier
Institut de Physique du Globe de Paris,
4 place Jussieu, 75005 Paris, France

(Mangiarotti et al. 2001), but non-tidal loading effects are not yet recommended for operational GNSS data processing (Ray et al. 2007; see http://www.bipm.org/utls/en/events/iers/Conv_PP1.txt). Further comparisons with space geodetic results are still needed to validate the models and to develop optimal strategies to attenuate systematic loading effects without introducing excessive modeling errors.

GPS, SLR, VLBI, and DORIS position time series are expected to show similar variations if position time series are computed in the same reference frame and if the loading signatures are significant compared to measurement errors. However, technique-specific systematic errors limit the empirical correlations so far. For example, GPS geocenter motion inferred from the network shift approach is not in agreement with expected values (Lavallée et al. 2006). A simple frame transformation is commonly used to remove global biases that affect all the station positions. A tri-dimensional similarity equation can be used to express station positions with respect to an external reference frame, usually the International Terrestrial Reference Frame (ITRF) or a related frame, by (where negligibly small non-linear terms have been dropped)

$$X^i(t) = T(t) + (1 + \lambda(t)) \cdot [X_r^i(t_0) + \dot{X}_r^i \cdot (t - t_0)] + R(t) \cdot [X_r^i(t_0) + \dot{X}_r^i \cdot (t - t_0)] + \delta^i \quad (1)$$

where X^i is the estimated position of station i at the epoch t , X_r^i is its position in the reference frame expressed at the epoch t_0 and \dot{X}_r^i is the corresponding velocity, δ^i is the noise term and T , R and λ are the transformation parameters, respectively, the translation vector, the anti-symmetric rotation matrix and the scale factor at the epoch t . This transformation is also the basis for the minimum constraint equations that are sometimes used to invert normal equation systems in order to estimate station coordinates with space geodetic techniques: orientation should normally be constrained for all techniques, as well as the origin for VLBI.

It is known that applying such a transformation affects non-linear variations of the estimated time series of station coordinates (Blewitt and Lavallée 2000; Tregoning and van Dam 2005; Collilieux et al. 2009). Indeed, as the ITRF is a long-term frame (Altamimi et al. 2007), the station position seasonal variations can partly alias into the transformation parameters. This effect is not desired and can be problematic for many applications: comparison with loading models, inversion to estimate loading mass density distributions, or comparison of space geodetic results from different techniques. The aim of this paper was to quantitatively describe this aliasing effect and to review and evaluate procedures that could be used to reduce it. Section 2 describes the synthetic data that are constructed to evaluate various suggested procedures. Section 3 assesses the results of the tests carried out on the synthetic data to show the performances of the

methods. And finally Sect. 4 applies the procedures to real GPS solutions in order to compare GPS displacements with loading models.

2 Strategy

2.1 Method to compute position time series

This section recalls the most general method that can be used to compute position time series in an homogeneous reference frame from a set of daily/weekly solutions.

First, a long-term reference frame $X_{\text{ref}}(t)$ is needed. It is recommended to recompute long-term positions and velocities for every station or for a subset of reliable stations from its own set of solutions and not to use directly an external reference frame designated by $X_r^i(t_0) + \dot{X}_r^i \cdot (t - t_0)$ in Eq. (1). At this step, discontinuities should be identified in the position time series and modeled in the estimated long-term frame $X_{\text{ref}}(t)$. The estimated long-term coordinates should be referred to the adopted long-term reference frame datum, for example, the ITRF, using stations showing the same discontinuity list. This step is necessary to avoid possible errors in the adopted long-term frame or inconsistencies with the input dataset which may affect transformed position time series. Second, the transformation parameters should be estimated between each daily/weekly solution and the estimated long-term coordinates of the epoch using Eq. (1). The next section will discuss different strategies for this purpose. Finally, detrended residuals $\Delta_d X^i(t)$ can be computed as follows:

$$\Delta_d X^i(t) = X^i(t) - X_{\text{ref}}^i(t) - [\hat{T}(t) + \hat{R}(t) + \hat{\lambda}(t) \cdot I_3] \cdot X_0^i(t) \quad (2)$$

where $X_0^i(t)$ are approximated coordinates of station i whereas the position time series w.r.t. the external reference frame $X_{\text{ex}}^i(t)$ can be computed as follows:

$$X_{\text{ex}}^i(t) = X^i(t) - [\hat{T}(t) + \hat{R}(t) + \hat{\lambda}(t) \cdot I_3] \cdot X_0^i(t) \quad (3)$$

The first two steps can be merged into one single step as done in the CATREF software (Altamimi et al. 2007). However, less flexibility is allowed for the estimation of the transformation parameters. We will specifically discuss here the second step which consists of estimating transformation parameters. The differences between the various methods will be highlighted using synthetic data.

2.2 Synthetic data and tests

We have simulated GPS weekly station position sets as follows:

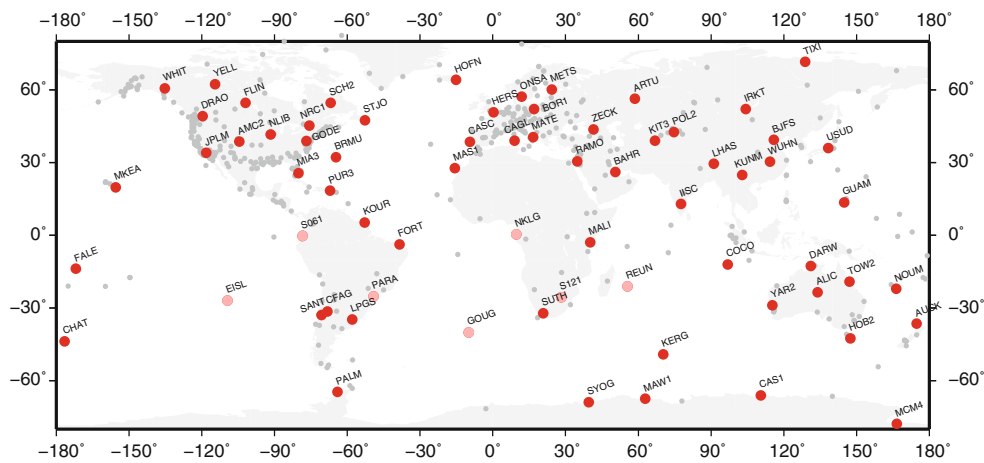


Fig. 1 Map of the MIT network (dots). The well-distributed sub-network is shown with larger colored dots. The stations of that sub-network that did not fill the requirement of at least 80% of estimation positions over the 11 years are highlighted in pink

$$X^i(t) = X_{\text{itr2008}}^i(t_0) + (t - t_0) \cdot \dot{X}_{\text{itr2008}}^i + \Delta_{\text{load}}^i(t) + \delta^i(t) \tag{4}$$

where $X^i(t)$ is the position vector of the station i at epoch t , $t_0 = 2005.0$ is the reference epoch of ITRF2008, $\Delta_{\text{load}}^i(t)$ is the loading displacement in the Center of Figure (CF) frame and $\delta^i(t)$ is a spatially correlated noise term. Station positions have been generated from 1998.0 to 2008.0, comprising 512 weeks. The real GPS network of the Massachusetts Institute of Technology (MIT) analysis center (MIT reprocessed solution), which is the most inclusive of all the reprocessed GPS solutions, has been adopted and station positions have been simulated only when station parameters were available in their SINEX files. The full network is composed of 748 stations, see Fig. 1, with many stations concentrated in North America and Europe. We restricted our simulations to the 441 GPS stations of the ITRF2008. The vector of spatially correlated noise $\delta(t)$ has been simulated from the full covariance matrices of the MIT solutions. Time-correlated noise processes are not mandatory here since we want to study systematic effects, so they have been ignored. The loading displacement model $\Delta_{\text{load}}^i(t)$ has been computed as the sum of three loading displacement models. They have been generated using the Green’s function approach and the load Love numbers of Han and Wahr (1995). The first includes the effect of the atmosphere at a 6-h sampling rate according to the model of the National Center for Environmental Prediction surface pressure. The second is derived from the ECCO Ocean Bottom Pressure (OBP) model at a sampling rate of 12h (Stammer et al. 2002). The third model, GLDAS, predicts the hydrological effect at monthly intervals (Rodell et al. 2004). These models have been averaged or interpolated to weekly spacing before being merged. They specifically show power at the seasonal frequencies and especially the annual (Ray et al. 2008).

2.3 Description of tests

Synthetic data sets computed from Eq. (4) have been analyzed as if they were real data. We estimated the transformation parameters between the position set of week t and a long-term reference frame expressed with respect to the ITRF2008 preliminary solution (Altamimi et al. 2011). With real data, estimated transformation parameters are non-zero due to apparent geocenter motion (combination of Center of Mass (CM) displacement with respect to CF due to loads and systematic errors), conventional orientation of the weekly frame, GPS scale dependency with the satellite and ground antenna phase center offsets and variations, noise, and aliasing effects related to loading. No frame error has been introduced in Eq. (4) to construct the synthetic data, which means that estimated translation, rotation, and scale parameters from synthetic solutions only reflect noise and aliasing terms. Figure 2 shows the transformation parameters estimated from the synthetic data in what will hereafter be designated the *standard* approach: all the transformation parameters are estimated with all available stations. Significant aliased annual signals can be seen, especially in the X and Z translation components, in the scale factor, and also in the rotations. The additional noise variations in 2006 are related to large variations of the variance of some point positions around the time of the 2004-12-26 Sumatra earthquake; station SAMP (Indonesia) is the most affected. We have determined that this extra noise does not change the conclusions shown here.

The columns of Table 1 designate the strategies that are tested here to reduce the aliasing error. Instead of using the whole set of available stations to estimate the transformation parameters, strategy *subnet* consists of using a well-distributed subset of stations to compute the transformation parameters. Indeed, loading effects are spatially correlated

Fig. 2 Transformation parameters estimated from synthetic data computed with the whole network of stations (*standard*). **a** X-translation, **b** Y-translation, **c** Z-translation, **d** scale factor (value in ppb scaled by 6.4), **e** X-rotation, **f** Y-rotation, **g** Z-rotation

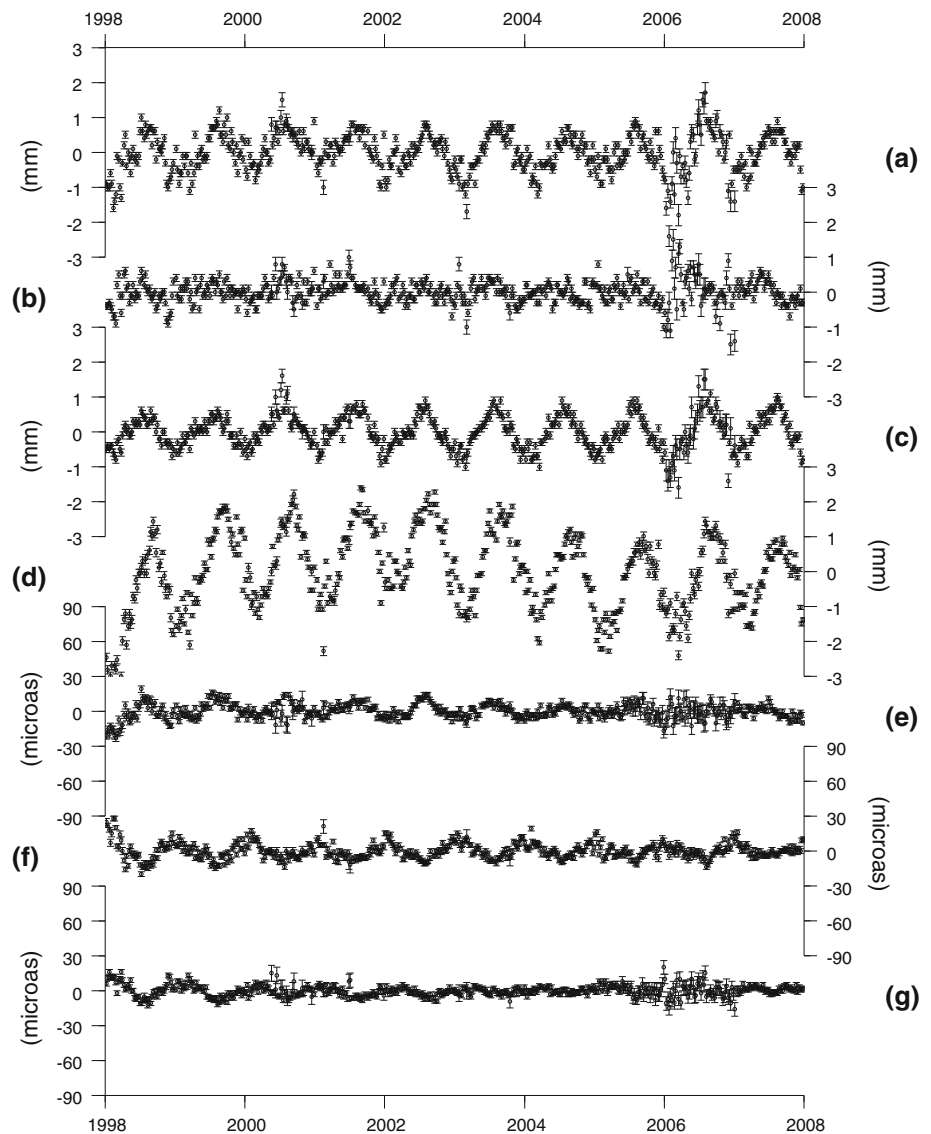


Table 1 Strategies used in this study to estimate the transformation between a weekly/daily frame and a long-term frame

Options	<i>Standard</i>	<i>Subnet</i>	<i>Downfull</i>	<i>Downdiag</i>	<i>Loadmod</i>	<i>Loadest</i>
Stations used	All	Well distributed sub-network	All	All	All	All
Weight matrix	Full	Full	Full, Height downweighted	Diagonal, Height downweighted	Full	Full
Loading corrections	No	No	No	No	Yes	No
Load parameters	No	No	No	No	No	Up to degree 5

and extracting a subset of stations is useful to avoid over-weighting those areas with a high station density, which accentuates the aliasing effect. Stations of the sub-network are chosen to have at least 80% of the full 11-year period covered by data and a limited set of discontinuities with segments longer than 20%. We followed the approach suggested by Collilieux et al. (2007) to remove stations in dense areas thus ensuring a globally uniform distribution. However, we

had to preserve some stations in poorly covered areas that did not exactly match the above criteria, specifically in the southern hemisphere, see Fig. 1.

It is also worth noting that the loading signals have larger amplitude in the height than in the horizontal components (Farrell 1972). With respect to the 7-parameter transformation, loading effects can be considered as biases, which are therefore more important in the height, since they are not

modeled. As a consequence, downweighting the height measurements has been suggested to reduce the aliasing effect (T. Herring, personal communication, 2009). This approach is already implemented in the Globk software (Herring 2004). There are several ways to implement this downweighting. We tested two approaches. First, we chose to use the inverse of the diagonal covariance matrix of the solution to weight the transformation but we modified the height formal error by a scaling factor (1.5 or 3.0). This approach is hereafter designated as *downdiag*. However, the off-diagonal terms of the covariance matrices contain significant statistical information, which is important to preserve. As a result, we also implemented the downweighting of heights while preserving the correlation terms of the covariance matrices following Guo et al. (2010). We first compute the covariance D_l in the local frames from the covariance matrix D by $D_l = R \cdot D \cdot R^t$ where R is a block-diagonal matrix composed by the rotation matrices from the global to the local frame for every station. We note $\sigma_e^i, \sigma_n^i, \sigma_u^i$ the standard deviations of the positions of station i along the East, North and Up component, and C the associated correlation matrix. The new downweighted covariance matrix D_{down} is given by

$$D_{\text{down}} = R^t \cdot \text{diag}(\sigma_e^1, \sigma_n^1, \alpha \cdot \sigma_u^1, \dots, \sigma_e^m, \sigma_n^m, \alpha \cdot \sigma_u^m) \cdot C \cdot \text{diag}(\sigma_e^1, \sigma_n^1, \alpha \cdot \sigma_u^1, \dots, \sigma_e^m, \sigma_n^m, \alpha \cdot \sigma_u^m) \cdot R$$

where α is the downweighting factor and m the number of stations. This dataset will be referred to as *downfull*.

Another way to handle this problem is to change the frame transformation model to include information about the loading displacements:

$$X^i(t) = T(t) + (1 + \lambda(t)) \cdot [X_r^i(t) + \Delta_{\text{load}}^i(t)] + R(t) \cdot [X_r^i(t) + \Delta_{\text{load}}^i(t)] + \delta_{\text{stat}}^i \tag{5}$$

It allows accounting for the non-linear variations of the reference frame. This approach is hereafter named *loadmod*. It has been shown to be equivalent to correcting daily/weekly station positions by the model prior to estimating the transformation parameters (Collilieux et al. 2010a).

Finally, we test the degree-1 deformation approach suggested by Lavallée et al. (2006), equation (A6–A7), which consists of estimating the low degree spherical harmonics of the load mass density that generates the deformation field simultaneously with the transformation parameters, hereafter called *loadest*. Those authors were, however, interested in the degree-1 terms of the load surface density whereas we focus here on the transformation parameters. Please note that there is an error in equation (A7) of that paper: $\left(\frac{3}{h'+2l'} - 1\right)$ should be replaced with $1 / \left(\frac{h'+2l'}{3} - 1\right)$.

It is worth noting that in all these approaches, the frame scale factor, λ , in Eq. (1) may or may not be estimated.

2.4 Evaluation of the aliasing error

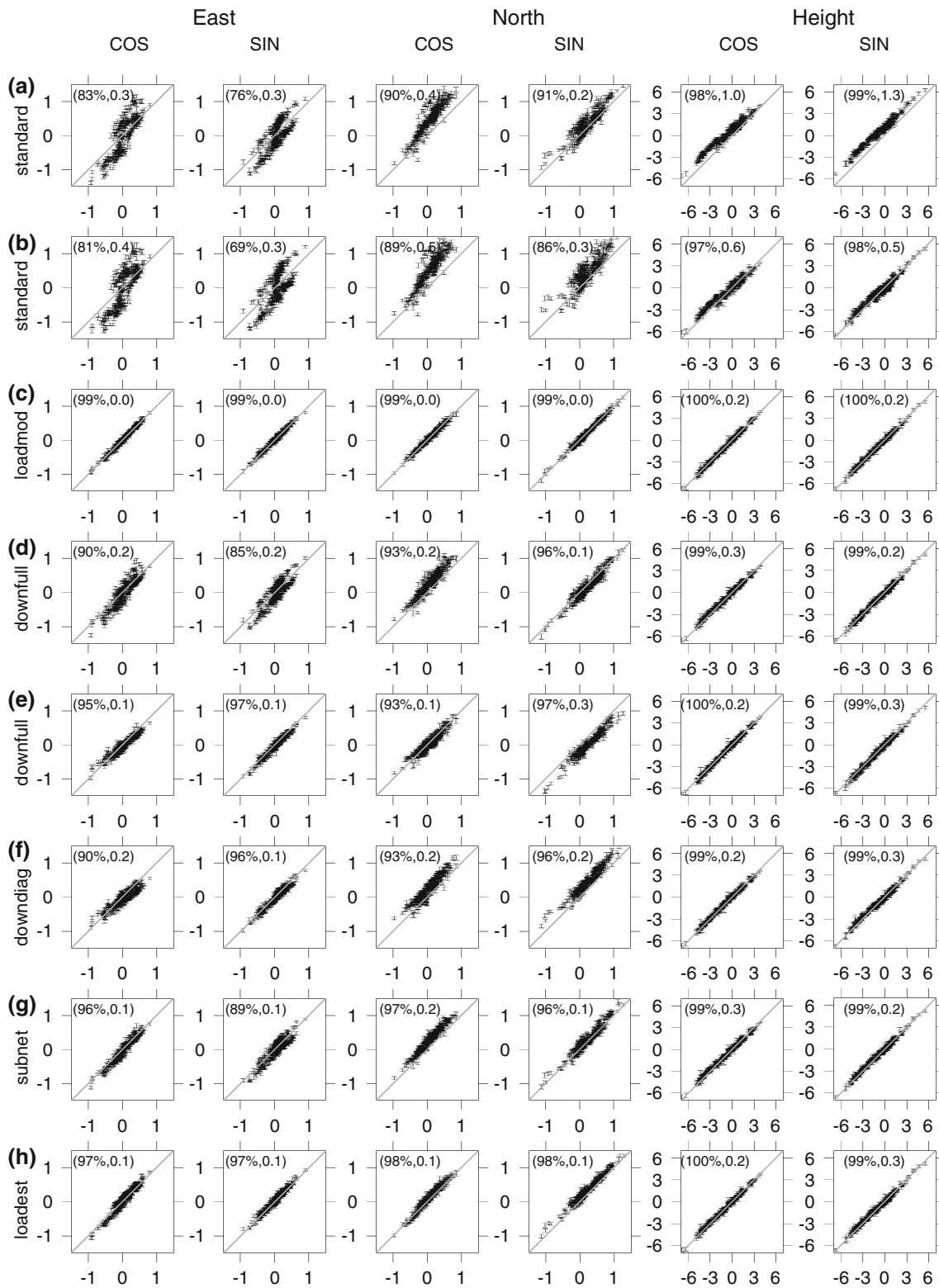
The outputs of all the processing methods described above are the epoch by epoch transformation parameters. Once they are computed, they can be incorporated into Eqs. (2) or (3) to compute the residuals of the station positions for every station. When synthetic data are processed, it is possible to quantify the effectiveness of each of the methods by checking how close the estimated transformation parameters are to zero. As their effect on station positions is different from one site to another, we also compare the station position residuals to the loading displacements that have been used to create the synthetic data.

Note that the Weighted Root Mean Squares (WRMS) of the differences for station positions are dominated by noise. As a consequence, these statistics are not useful for evaluating the aliasing effects. As the loading effects have a large signal at the annual frequency, see Fig. 2, we choose to evaluate each method on its ability to properly recover the loading signals at the annual frequency in the station position time series.

3 Evaluation of the methods

3.1 Scale

Not estimating the scale in the frame transformation has been recommended by several authors (Tregoning and van Dam 2005; Lavallée et al. 2006). Indeed, as can be noted in Fig. 2d, a large annual signal is observed in the scale when it is estimated in the *standard* approach. Inter-annual variations are also visible; they are mostly attributed to continental water loading (van Dam et al. 2001). Figure 3a shows, for all stations with sufficient data (more than three years), the comparison between the in-phase and out-of-phase terms of the annual signals estimated in the station position time series residuals [computed according to Eq. (2)] and the annual signals estimated in the loading models used to generate the data. The more closely the points are located on the diagonal, the more satisfactory the transformation. It is interesting to note the systematic behavior of the annual signal. Most of the terms are over-estimated using the *standard* method, except the East component. The bimodal distribution noticed in the East component can be explained by an aliasing in the X-translation for the out-of-phase term and an aliasing of the X-translation and rotations for the in-phase term. The effect of the rotations tends to increase the error in South America and decrease the X-translation aliasing in Siberia. As could be expected, the height component is the most affected, especially the out-of-phase term which is biased by about 1 mm. If the scale is not estimated, see Fig. 3b, the picture is almost unchanged for the horizontal components but the height annual signals are obviously better recovered.



◀ **Fig. 3** Comparison of the annual signal estimated in the residuals of the frame transformation as defined in Sect. 2.3 applied to synthetic data (Y -axis), and the annual signal estimated in the loading model that has been used to generate the synthetic data (X -axis) in millimeters. In-phase term (COS) and out-of-phase term (SIN) are presented for the East, North and Height components from the left to the right for the different strategies presented in Sect. 2.2. **a** *standard*, scale estimated; **b** *standard*, scale not estimated; **c** *loadmod*, scale estimated; **d** *downfull* height standard deviations multiplied by 1.5; **e** *downfull* height standard deviations multiplied by 3.0; **f** *downdiag* height standard deviations multiplied by 3.0; **g** *subnet*; **h** *loadest*. Scale factors have not been estimated for **d** to **h**. Numbers inside the brackets for each plot are the correlation coefficient and the WRMS of the differences in millimeters

Figure 4a, b shows the aliased loading signal in the translations and scale factors for these two cases. The translation parameters are almost unchanged when the scale factor is not estimated since the GPS network almost covers the whole globe.

Collilieux et al. (2010b) showed that the annual variations observed in the GPS scale factor can be partly explained by our loading model, but not completely. However, the scale behavior is quite stable in time so that it is reasonable to estimate one constant scale factor for the whole period of time. This can be done in a one-step run if all the transformation parameter time series are estimated simultaneously or in a two-step approach by applying first the mean scale factor to the reference solution. A 6-parameter transformation (no scale) can then be estimated.

Unfortunately, most of the methods presented above cannot fully solve the problem of aliasing in the scale factor if one scale factor is estimated per solution. The method consisting of incorporating the loading model in the transformation (*loadmod*) performs nicely, see Figs. 3c and 4c, but only if the loading perfectly fits the GPS data (see Sect. 4 for discussion). It is possible to reduce the annual signal in the scale when using a well-distributed network of stations for the frame transformation, as discussed by Collilieux et al. (2007). However, the performance of the method is variable and depends strongly on the sub-network. Indeed, we did not notice a reduction in the annual scale amplitude when studying our MII well-distributed sub-network either with synthetic or real data. Only the estimation of the deformation field, as already discussed by Lavallée et al. (2006), seems to decrease significantly the scale factor annual signal (see Sect. 3.4) but does not nullify it.

As a consequence, we will discuss the following results in the case of a 6-parameter frame transformation. The scale issue will be discussed further for the strategy *loadest* only.

3.2 Downweighting height

Transformation parameters obtained with the *standard* approach have been computed using the full covariance matrix of the solutions. It is worth noting that GPS height

determinations are about 3 times less precise than the horizontal ($\sigma_{up} \approx 3 \cdot \sigma_{north}$), which means that the height component is naturally downweighted in the *standard* approach.

Figure 3d–f shows the results obtained when the whole network of stations is used to compute the transformation parameters while applying downweighting of the heights (no scale estimated here). The only difference with Fig. 3b is the weighting. Three different downweighting strategies are shown. Height uncertainties were multiplied by 1.5 ($\sigma_{up} \approx 5 \cdot \sigma_{north}$) or by 3.0 ($\sigma_{up} \approx 10 \cdot \sigma_{north}$) but the correlations were preserved, Fig. 3d, e. Correlations were canceled in Fig. 3f ($\sigma_{up} \approx 10 \cdot \sigma_{north}$). It can be clearly noticed that downweighting the heights has a positive effect on the horizontal components. When the height weight is slightly decreased, the pattern of the annual is close to the *standard* case but the error has been significantly mitigated. Even the height agreement is improved with estimated correlations larger than 99% and mean deviations smaller than 0.3 mm for the in-phase and out-of-phase terms. When the height weight is decreased further, see Fig. 3e, the agreement improves. Indeed, the translation parameters along the X - and Y -axes become smaller, see Fig. 4d, e. However, there is a difference depending on whether the correlations are used or not in the weighting. The recovered annual term in the North component is different, compare Fig. 3e and f, which is related to the differences in the X - and Z -translations, see Fig. 4e and f. The out-of-phase term is generally under-estimated in the full-weighting case whereas the in-phase term is slightly over-estimated. However, the error is reasonable for both methods when synthetic data are studied. We also tried to decrease the height weight even more but the general level of agreement between the residuals and the true values did not improve significantly.

3.3 Using a sub-network

Restricting the transformation to a subset of stations is the most natural way to proceed. This is what is commonly done when some station coordinates that are weakly determined are rejected from the transformation estimation (with a simple outlier rejection test). Additionally, using a well-distributed sub-network significantly reduces the transformation parameter biases. Our sub-network, shown on Fig. 1, is composed by 77 stations, selected following the criteria defined above. Figures 3g and 4g show the performance of the method. The biggest bias in the residual position time series is observed in the in-phase annual term of the north component and in the out-of-phase term of the east component. The average error at the annual frequency is within 0.2 mm WRMS for this term which shows that the approach is reliable for mitigating aliasing effects. Aliased annual signals are reasonably small in the translation parameters although signal along the Z -axis is still visible. When the height is downweighted conjointly by 1.5, the aliasing errors decrease

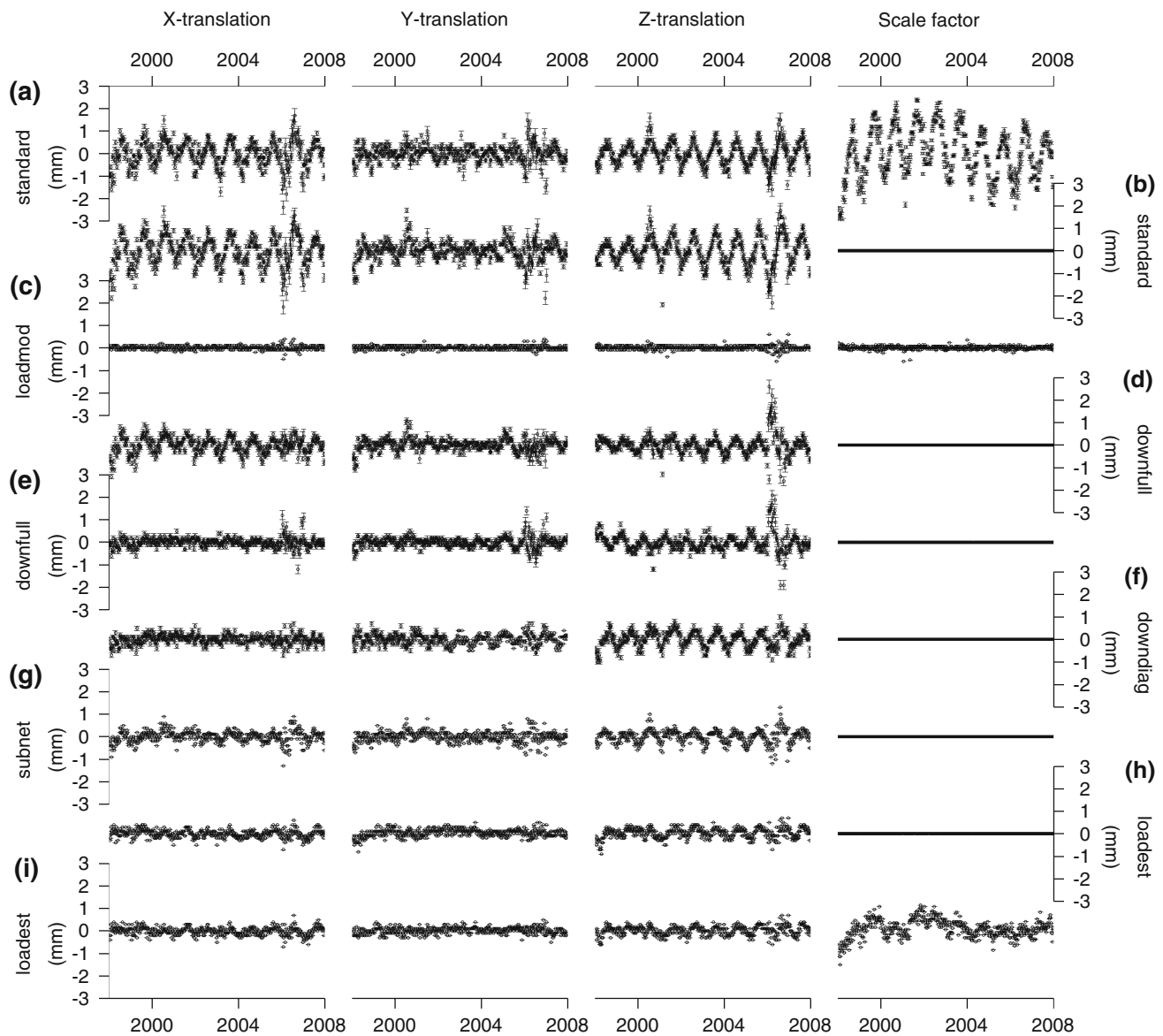


Fig. 4 Translations along the X-, Y- and Z-axis in millimeters and scale factors in millimeters (ppb value multiplied by 6.4) estimated between the synthetic weekly frames and the long-term frame. A different strat-

egy has been used for each row. See the legend of Fig. 3 for rows **a** to **h**. Strategy used for row **i** is identical to row **h** except that the scale factor has been estimated also

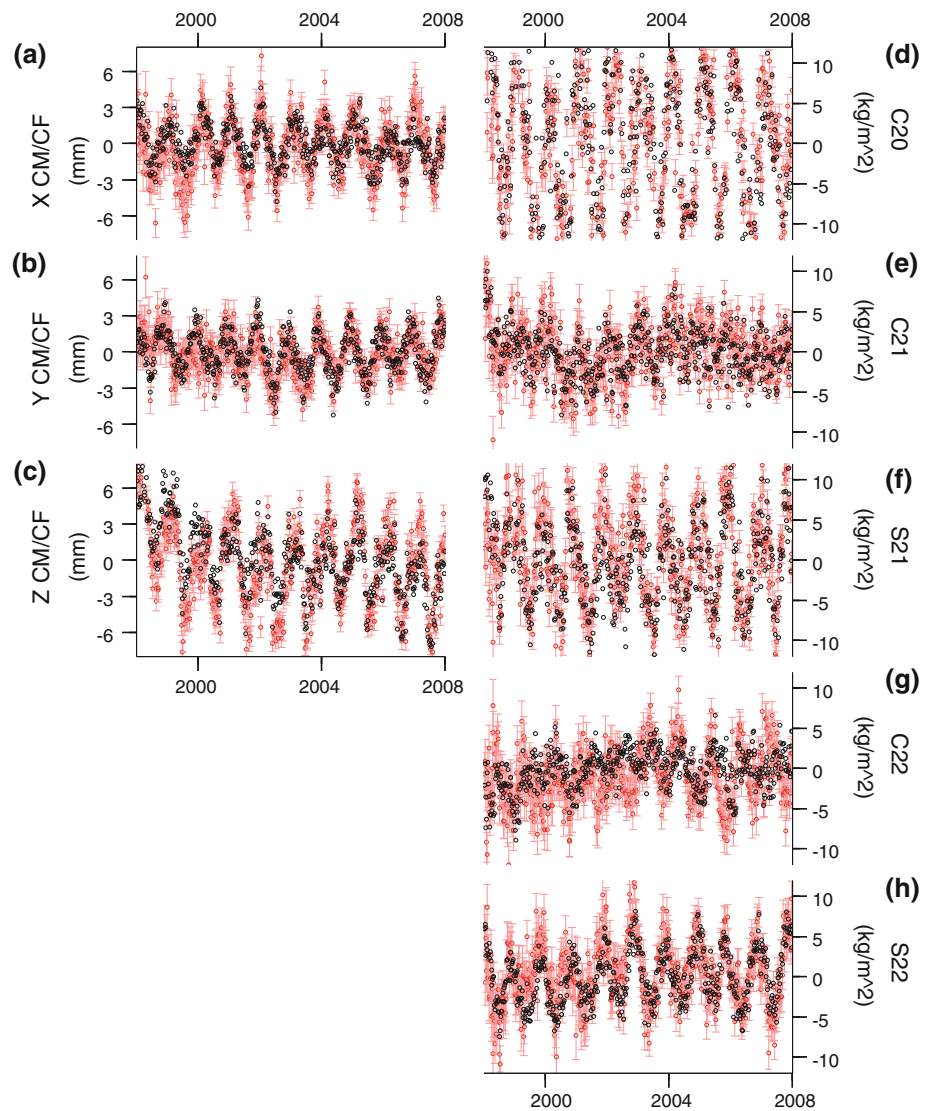
but only by 0.1 mm annual WRMS in the in-phase terms of the annual signal for the north and height components. For this particular weighting, it is better to use a subset of stations rather than the full network. When the height uncertainty is multiplied by 3.0, the effect of the downweighting tends to dominate which means that using either the sub-network or the full network give similar results.

3.4 Estimating the deformation field

We have seen from the results above that using a loading model in the transformation is effective. The main limitation is the loading model accuracy and possible GPS systematic

errors, but another limitation is the availability of the loading model itself. Estimating the displacements caused by the loading of the Earth's crust is an alternative. However, due to the spatial distribution of GPS sites, it is only possible for the longest wavelengths of the deformation field. Following Wu et al. (2003), we only estimated the load surface density coefficients up to spherical harmonic degree five. We also paid attention to model the deformation field in the CF frame, by adopting the degree-1 load Love numbers in the CF frame (Blewitt 2003), in order to estimate a translation that relates the ITRF origin to the GPS frame origin. Indeed, modeling the deformation field in the Center of Network frame (Wu et al. 2002) would have had no effect on reducing the

Fig. 5 Estimated normalized surface mass density coefficients of degree 1 and 2 using strategy *loadest* and a truncation degree equal to 5 are shown in red with their $1-\sigma$ formal errors (no scale estimated). These results have been obtained using synthetic GPS data. The true load coefficients are shown in *black*. Degree-1 coefficients have been converted into geocenter motion using equation 1 of Collilieux et al. (2009)



aliasing. Further modeling the deformation field in the CM would have removed the geocenter motion contribution from the estimated translation, which is not desired.

For comparison with the other approaches, we first plotted the results when the scale was fixed to zero. Figure 5 shows the estimated surface mass density coefficients from synthetic data for a truncation degree equal to five. It can be noticed that the estimated coefficients are consistent with the expected values. Although only the low degrees are estimated, Figs. 3h and 4h show that the method is effective at reducing the aliasing effect. It performs better than any other in the horizontal and is as effective in the height. Please note that the full covariance matrix has been used with no modification of the stochastic model. The full network of stations is also used, except those that have been identified as outliers in the least squares estimation process.

We also estimated the scale factor in the frame transformation as a test. The aliasing effect depends on the truncation degree of the spherical harmonic expansion of the load density. We noticed using the synthetic data that the scale factor annual signal amplitude becomes smaller than 0.2 mm for degree three up to degree six, see Fig. 6. Figure 4i shows, for example, the estimated scale factor for a truncation degree of five. The variations of scale, compared with Fig. 4a are drastically reduced, but inter-annual variations are not removed. We noted a larger annual signal in the scale factor estimated from real data with an amplitude of 0.6 ± 0.1 mm for a truncation degree equal to five. This is, however, much smaller than the amplitude estimated in the standard approach which is 1.6 mm. If the estimation of the scale is needed, this approach is relevant but does not fully solve the aliasing issue, especially at the inter-annual frequencies, see Fig. 4i.

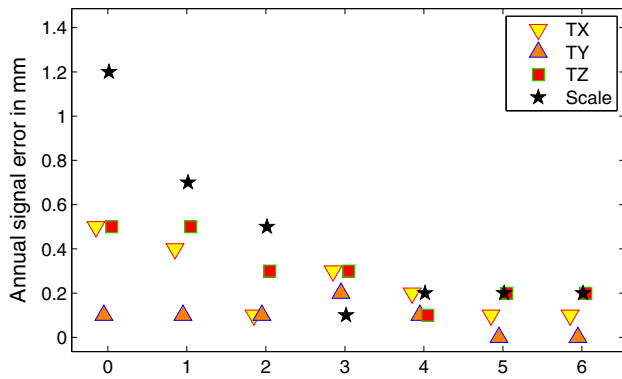


Fig. 6 Aliased annual signal amplitudes in the translation and scale factor (ppb value multiplied by 6.4) estimated using the strategy *loaddest* as a function of the truncation degree of the deformation field. These results have been obtained using synthetic GPS data

3.5 NNR-condition

Above, we discussed the 7-parameter transformation that is used to constrain the frame origin, orientation, and scale. However, GPS is theoretically sensitive to the origin and scale of the frame so that only the orientation must be defined in principle. Constraining a normal matrix with the standard minimum constraint approach is equivalent to performing a uniformly-weighted transformation between a conventionally oriented frame and the output frame. As a consequence, this constraint should affect the loading signal as well, but to a lesser extent since only orientation is considered. We performed the same computation as above but estimating only the rotation parameters when using the full network of stations (*standard*) or a well-distributed sub-network (*subnet*). Aliased loading effects in the rotation parameters show repeatabilities smaller than $5.6 \mu\text{as}$ in any cases, which is about 0.15 mm. However, the annual signal amplitude in the X and Y component is divided by about 2 to reach 2.3 and $3.8 \mu\text{as}$, respectively when a sub-network is used. As a consequence, the impact on the position time series is quite small. The worst determined term is the in-phase annual term in the North component for both *standard* and *subnet* strategies. While the correlation and WRMS of the in-phase North term with respect to the true values are 86% and 0.2 mm for the standard case, they are, however, 96% and 0.1 mm when a well-distributed sub-network is selected for the NNR condition. As a consequence, a well-distributed network is required for applying the NNR-condition and to recover annual signals in the horizontal at the level of 0.1 mm WRMS.

4 Application to real data

In this section, we applied the approaches described above to real GPS position time series to see if the agreement

between the GPS position time series and our loading model is improved compared with the *standard* approach. Figure 7 is similar to Fig. 3, except that the annual signal plotted on the Y-axis comes from the analysis of the MII GPS data. The X-axis still shows the annual signal estimated in the loading model over the period 1998.0-2008.0. Such a plot represents the level of agreement between GPS products and the loading model at the annual frequency, depending on the approach adopted to define the frame origin, orientation and scale. Figure 7a shows the *standard* approach when the scale is estimated, as a reference. A clear bias can be observed, especially for the out-of-phase terms in the height, as seen with the synthetic data. As a consequence, for all the results that are shown next, the scale factor is not estimated. We also show in Fig. 8a the translations and scale factor estimated for the *standard* approach. Figure 8b–f shows the differences between the estimated translations for alternative approaches and the *standard* approach.

Using the loading model in the transformation (*loadmod*), cf. Figure 7b, does not show any better agreement between GPS and the loading model compared with any of the other methods: using a sub-network for the frame transformation (*subnet*), Fig. 7c, downweighting height (*downfull*), Fig. 7d, e or estimating the deformation field (*loadest*), Fig. 7f. This shows that discrepancies between GPS displacements and the loading models are not related to the aliasing effects. It can be noticed in Fig. 8 that translation differences with the *standard* approach reach about 1 mm at the annual frequency in the X- and Z-axes. As observed with synthetic data, the agreement between the GPS North component annual term and the loading model is better when the aliasing is reduced. The *loadest* approach seems to perform slightly better than any of the other approaches. Indeed, the WRMS of the differences of annual signals (in-phase and out-of-phase terms) and their correlations are smaller in all the components except the out-of-phase term in the North component. However, the fit with the loading model is satisfactory for the three other approaches. Nonetheless, caution should be used when interpreting the results of the *downfull* strategy. The North annual out-of-phase terms recovered when the height uncertainty is multiplied by three seem to be under-evaluated compared with any other approaches. This is not the case when the height uncertainty is multiplied by 1.5. This was not so obvious for the synthetic data although it was visible. We notice that this effect is related to larger differences in the Z-translation annual signal, see Fig. 8e. As a consequence, using an uncertainty scaling factor of 1.5 or using diagonal weight only is preferred. We think it is always better to leave the stochastic model unaffected, which is why we favor using either a well-distributed network for the frame transformation or estimating the low-degree coefficients of the deformation field simultaneously.

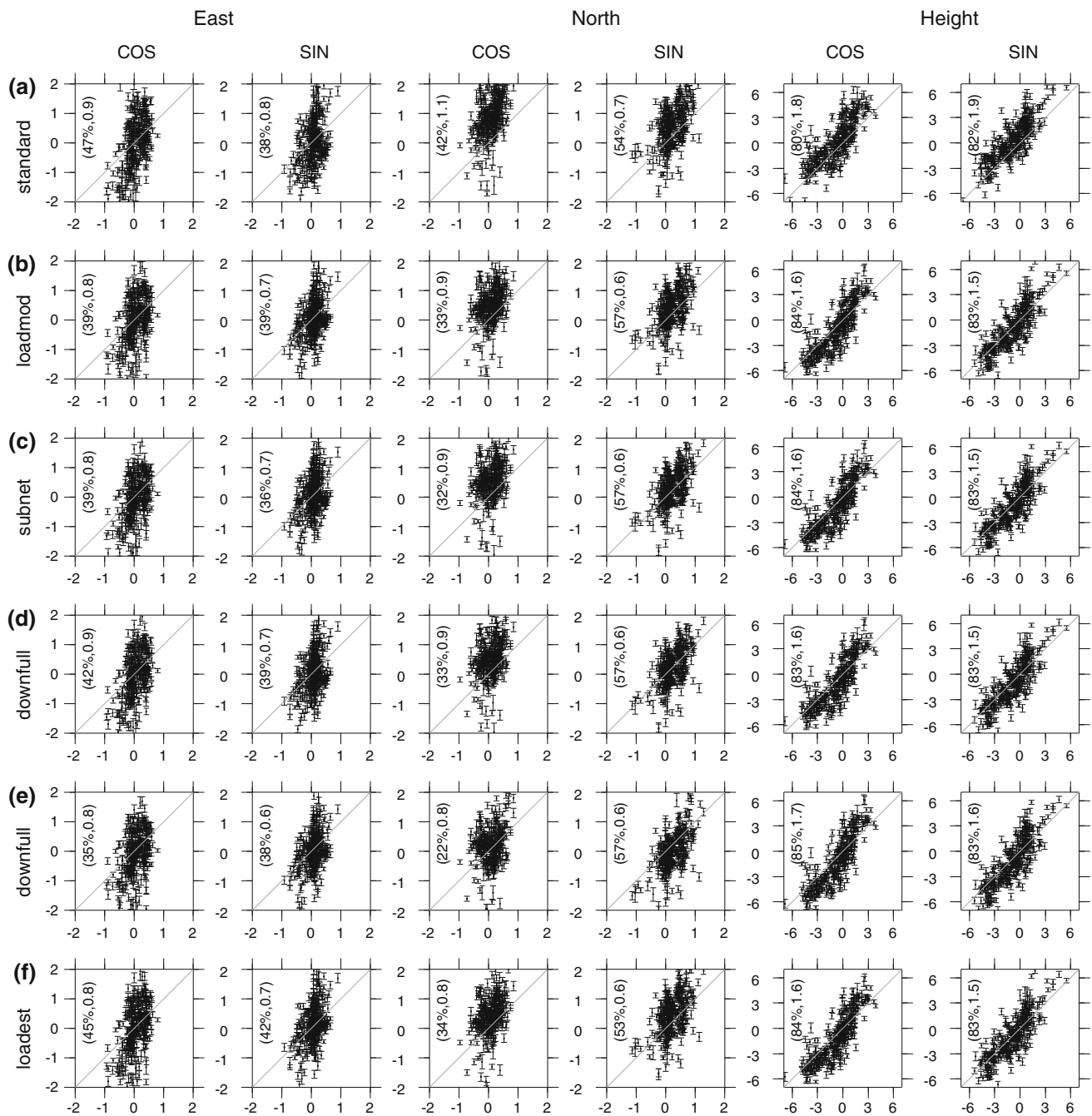


Fig. 7 Comparison of the annual signal estimated in the residuals of the frame transformation as defined in Sect. 2.3 applied to real data (Y-axis), and the annual signal estimated in the loading model (X-axis) in millimeters. **a** *standard*, scale estimated; **b** *loadmod*; **c** *subnet*;

d *downfall* height standard deviations multiplied by 1.5; **e** *downfall* height standard deviations multiplied by 3.0; **f** *loadest*. Scale factors have not been estimated for **b** to **f**. Same legend as Fig. 3

5 Discussion

Lavallée et al. (2006) suggested two approaches for estimating the low degrees of the load mass surface density. We adopted here the so-called degree-1 deformation approach since we wanted to remove the absorbed loading signal in the translations while preserving the net-trans-

lation due to degree-1 in these parameters. In that case, translation and rotation parameters and the degree-1 of the mass surface density are estimated simultaneously as well as higher degree terms. The CM-approach consists of modeling the deformation field in the CM frame instead of the CF frame and estimating rotation parameters only since GPS is theoretically sensitive to CM. The two approaches lead to two

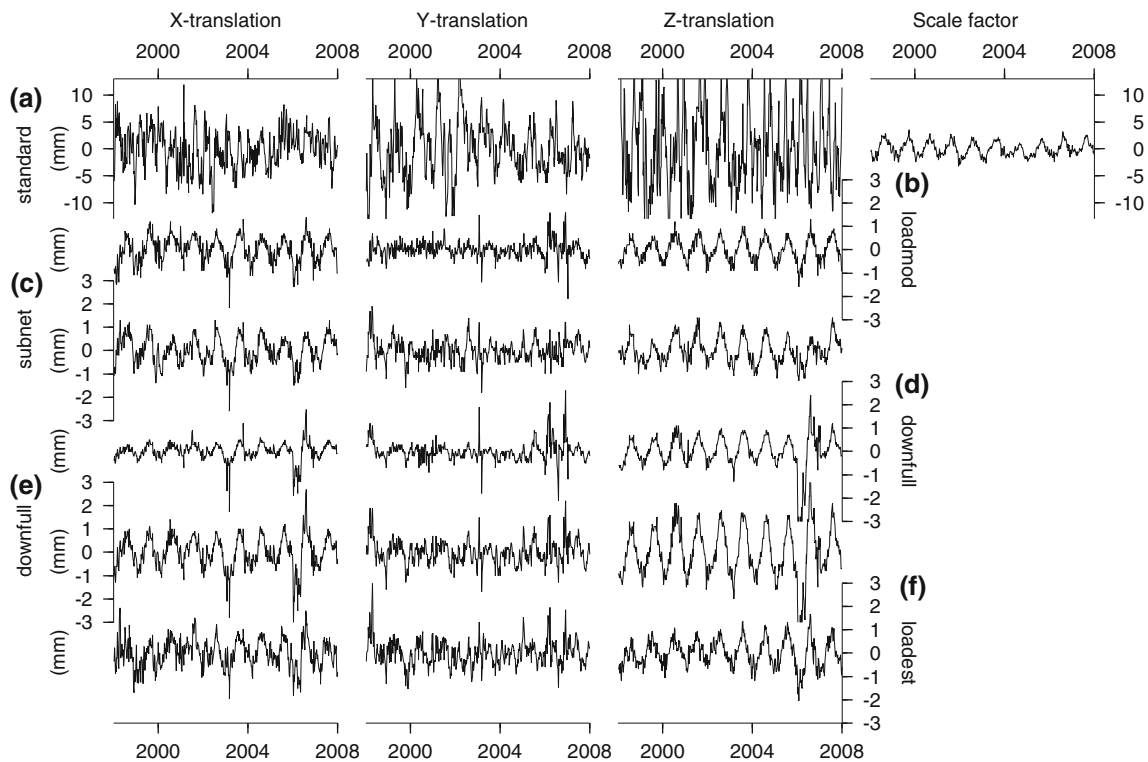


Fig. 8 a Translations along the X-, Y- and Z-axis in millimeters and scale factors in millimeters (ppb value multiplied by 6.4) estimated between the M1 weekly frames and the long-term frame. **b–f**

Differences between translation parameters estimated with tested strategies and those derived from the *standard* method shown in **a**. See the legend of Fig. 7

Table 2 Geocenter motion (CM w.r.t. CF) annual signal from the degree-1 mass surface density parameters estimated from the GPS M1 solutions with two different strategies (lines 1 and 2)

	X amplitude (mm)	X phase (degrees)	Y amplitude (mm)	Y phase (degrees)	Z amplitude (mm)	Z phase (degrees)
Degree-1 deformation approach	3.8 ± 0.3	48 ± 4	2.0 ± 0.2	3 ± 5	7.9 ± 0.5	38 ± 3
CM-approach	1.0 ± 0.2	71 ± 9	2.4 ± 0.2	310 ± 5	4.5 ± 0.3	51 ± 4
CM-approach (Fritsche et al. 2010)	0.1 ± 0.2	43 ± 93	1.8 ± 0.2	334 ± 11	4.0 ± 0.2	25 ± 3
GPS/GRACE/OBP (Collilieux et al. 2009)	1.3 ± 0.3	6 ± 14	3.0 ± 0.3	338 ± 6	4.6 ± 0.2	23 ± 3
Loading model (Collilieux et al. 2009)	2.1 ± 0.1	28 ± 2	2.1 ± 0.1	338 ± 2	2.7 ± 0.1	48 ± 2
Opposite of the translation from degree-1 deformation approach	0.4 ± 0.2	165 ± 30	3.6 ± 0.3	302 ± 5	4.4 ± 0.5	125 ± 7

Phase are supplied according to the model $A \cdot \cos(2\pi \cdot (t - 2000.0) - \phi)$ with t in years. Independent geocenter motion estimates are also reported (lines 3–5) as well as some values obtained from translation estimates (line 6)

distinct estimates of the mass surface density coefficient estimates. As an illustration, Table 2, lines 1 and 2, provides the annual signals estimated in the geocenter motion time series computed from the degree-1 coefficients (equation 1 of Collilieux et al. (2009)). Differences may reach up to 3.4 mm in the amplitudes and may exceed one month in phase. Our CM-approach solution agrees within 1 mm in amplitude and 1 month in phase with the reprocessed solution of Fritsche et al. (2010). For comparison, we also supplied two distinct models from Collilieux et al. (2009). The first is a forward loading

model and the second is the result of a global inversion using GPS, Gravity Recovery and Climate Experiment (GRACE) and OBP. Either of our two degree-1 estimations seems to agree better with these two loading models. However, the aliasing effect reduction using these two distinct deformation fields is only different at the level of 0.3 mm RMS for each translation component without clear seasonal patterns, thus validating the degree-1 deformation field approach used for the purpose of aliasing mitigation in this study. We also reported in Table 2 the opposite of the translation estimated

with the degree-1 deformation approach (sum of Fig. 8a and f). It can be observed that apparent reprocessed GPS geocenter motion is still not reliable, even with the aliasing effect removed.

Thanks to the different tests performed here, we are now able to draw some conclusions about the level of agreement between the GPS position time series and the loading model. Indeed, we can reasonably exclude the aliasing effect as being a major source of discrepancies. When looking at Fig. 7f, the following general comments can be formulated: The agreement of the annual signal in the Height component is good on average since all the points are located along the diagonal. The discrepancy is 1.6 mm WRMS for the in-phase term and 1.5 mm WRMS for the out phase term. In the horizontal, the loading model generally shows a smaller amplitude than the GPS and the agreement for the in-phase and out-of-phase terms of the annual signals is less than 0.8 mm for both components. These results are encouraging but the discrepancies are still quite important. The horizontal component signals of the GPS stations should be investigated further in the future studies, especially by comparing GPS results with different loading models and the results of the GRACE to better understand the origin of the discrepancies shown here.

6 Conclusion and recommendations

We reviewed the procedures that can be used to modify the origin, orientation, and scale of a time series of GPS frames. We paid attention to discuss the transformations that preserve the loading signals that are inherently contained in the station coordinates. This is especially important in order to interpret correctly the non-linear variations in the station position time series. Using synthetic data, we showed that the standard approach consisting of using the largest set of stations in the frame transformation is not optimal of whether the scale is estimated or not. The scale parameter should be definitively fixed to a constant value over time or its seasonal variations fixed to zero. But a rigorous approach is possible only if all the frame time series are analyzed in one unique estimation process. The benefit of using an alternative approach is especially important for the annual signals in the horizontal components. Downweighting height, restricting the station set to a well-distributed sub-network, or estimating the low-degrees of the load-surface density all perform well. The well-distributed network approach is the easiest to implement whereas the handling of the covariance terms is still to be defined when downweighting height. A slight advantage is given to the third method consisting of estimating the deformation field, which is almost free of any systematic bias according to our simulations. Thanks to this study, we were able to conclude that the aliasing effect is not the main source of discrepancy between GPS position time

series and the loading models. Annual signals are shown to agree at the 1.5 mm level WRMS in the height and the 0.8 mm level WRMS in the horizontal. Further studies are needed to understand the sources of the remaining inconsistencies.

Acknowledgments This work was partly funded by the CNES through a TOSCA grant. All the plots, except Fig. 6, have been made with the General Mapping Tool (GMT) software (Wessel and Smith 1991).

References

- Altamimi Z, Collilieux X, Legrand J, Garayt B, Boucher C (2007) ITRF2005: a new release of the International Terrestrial Reference Frame based on time series of station positions and Earth Orientation Parameters. *J Geophys Res* 112(B09401). doi:[10.1029/2007JB004949](https://doi.org/10.1029/2007JB004949)
- Altamimi, Z and Collilieux, X and Métivier, L (2011) ITRF2008: an improved solution of the International Terrestrial Reference Frame. *J Geodesy*. doi:[10.1007/s00190-011-0444-4](https://doi.org/10.1007/s00190-011-0444-4)
- Blewitt G (2003) Self-consistency in reference frames, geocenter definition, and surface loading of the solid Earth. *J Geophys Res* 108. doi:[10.1029/2002JB002082](https://doi.org/10.1029/2002JB002082)
- Blewitt G, Lavallée D (2000) Effect of annually repeating signals on geodetic velocity estimates. Tenth General Assembly of the WEGENER Project (WEGENER 2000), San Fernando, Spain, September 18–20
- Collilieux X, Altamimi Z, Coulot D, Ray J, Sillard P (2007) Comparison of very long baseline interferometry, GPS, and satellite laser ranging height residuals from ITRF2005 using spectral and correlation methods. *J Geophys Res* 112(B12403). doi:[10.1029/2007JB004933](https://doi.org/10.1029/2007JB004933)
- Collilieux X, Altamimi Z, Ray J, van Dam T, Wu X (2009) Effect of the satellite laser ranging network distribution on geocenter motion estimation. *J Geophys Res* 114(B04402). doi:[10.1029/2008JB005727](https://doi.org/10.1029/2008JB005727)
- Collilieux X, Altamimi Z, Coulot D, van Dam T, Ray J (2010) Impact of loading effects on determination of the International Terrestrial Reference Frame. *Adv Space Res* 45:144–154. doi:[10.1016/j.asr.2009.08.024](https://doi.org/10.1016/j.asr.2009.08.024)
- Collilieux X, Métivier L, Altamimi Z, van Dam T, Ray J (2010b) Quality assessment of GPS reprocessed Terrestrial Reference Frame. *GPS Solut*. doi:[10.1007/s10291-010-0184-6](https://doi.org/10.1007/s10291-010-0184-6)
- Farrell WE (1972) Deformation of the earth by surface loads. *Rev Geophys Space Phys* 10(3):761–797
- Fritsche M, Dietrich R, Rülke A, Rothacher M, Steigenberger P (2010) Low-degree earth deformation from reprocessed GPS observations. *GPS Solut* 14(2):165–175. doi:[10.1007/s10291-009-0130-7](https://doi.org/10.1007/s10291-009-0130-7)
- Guo J, Ou J, Wang H (2010) Robust estimation for correlated observations: two local sensitivity-based downweighting strategies. *J Geodesy* 84(4):243–250. doi:[10.1007/s00190-009-0361-y](https://doi.org/10.1007/s00190-009-0361-y)
- Han D, Wahr J (1995) The viscoelastic relaxation of a realistically stratified earth, and a further analysis of postglacial rebound. *Geophys J Int* 120:287–311. doi:[10.1111/j.1365-246X.1995.tb01819.x](https://doi.org/10.1111/j.1365-246X.1995.tb01819.x)
- Herring T (2004) GLOBK: Global Kalman filter VLBI and GPS analysis program version 4.1. Tech. rep., Massachusetts Institute of Technology, Cambridge
- Lavallée DA, van Dam TM, Blewitt G, Clarke PJ (2006) Geocenter motions from GPS: A unified observation model. *J Geophys Res* 111:5405. doi:[10.1029/2005JB003784](https://doi.org/10.1029/2005JB003784)
- Mangiarotti S, Cazenave A, Soudarin L, Crétaux JF (2001) Annual vertical crustal motions predicted from surface mass redistribution

- and observed by space geodesy. *J Geophys Res* 106:4277–4292. doi:[10.1029/2000JB900347](https://doi.org/10.1029/2000JB900347)
- McCarthy D, Petit G (2004) IERS Technical Note 32-IERS Conventions (2003). Tech. rep., Verlag des Bundesamts für Kartographie und Geodäsie, Frankfurt am Main, Germany. <http://maia.usno.navy.mil/conv2003.html>
- Petrov L, Boy J (2004) Study of the atmospheric pressure loading signal in very long baseline interferometry observations. *J Geophys Res* 109(B18). doi:[10.1029/2003JB002500](https://doi.org/10.1029/2003JB002500)
- Ray J, Altamimi Z, Collilieux X, Dam TMvan (2008) Anomalous harmonics in the spectra of GPS position estimates. *GPS solution* 12(1):55–64. doi:[10.1007/s10291-007-0067-7](https://doi.org/10.1007/s10291-007-0067-7)
- Rodell M, Houser PR, Jambor U, Gottschalck J, Mitchell K, Meng CJ, Arsenault K, Cosgrove B, Radakovich J, Bosilovich M, Entin JK, Walker JP, Lohmann D, Toll D (2004) The Global Land Data Assimilation System. *Bull Amer Meteor Soc* 85(3):381–394. doi:[10.1175/BAMS-85-3-381](https://doi.org/10.1175/BAMS-85-3-381)
- Stammer D, Wunsch C, Fukumori I, Marshall J (2002) State estimation improves prospects for ocean research. *Eos Trans AGU* 83(27):289–295. doi:[10.1029/2002EO000207](https://doi.org/10.1029/2002EO000207)
- Tregoning P, van Dam TM (2005) Effects of atmospheric pressure loading and seven-parameter transformations on estimates of geocenter motion and station heights from space geodetic observations. *J Geophys Res* 110:3408. doi:[10.1029/2004JB003334](https://doi.org/10.1029/2004JB003334)
- van Dam TM, Herring TA (1994) Detection of atmospheric pressure loading using very long baseline interferometry measurements. *J Geophys Res* 99:4505–5417. doi:[10.1029/93JB02758](https://doi.org/10.1029/93JB02758)
- van Dam TM, Blewitt G, Heflin MB (1994) Atmospheric pressure loading effects on Global Positioning System coordinate determinations. *J Geophys Res* 99:23939–23950. doi:[10.1029/94JB02122](https://doi.org/10.1029/94JB02122)
- van Dam TM, Wahr J, Milly PCD, Shmakin AB, Blewitt G, Lavallée D, Larson KM (2001) Crustal displacements due to continental water loading. *Geophys Res Lett* 28:651–654. doi:[10.1029/2000GL012120](https://doi.org/10.1029/2000GL012120)
- Wessel P, Smith WHF (1991) Free software helps map and display data. *EOS Trans* 72:441. doi:[10.1029/90EO00319](https://doi.org/10.1029/90EO00319)
- Wu X, Argus DF, Heflin MB, Ivins ER, Webb FH (2002) Site distribution and aliasing effects in the inversion for load coefficients and geocenter motion from GPS data. *Geophys Res Lett* 29(24):2210. doi:[10.1029/2002GL016324](https://doi.org/10.1029/2002GL016324)
- Wu X, Heflin MB, Ivins ER, Argus DF, Webb FH (2003) Large-scale global surface mass variations inferred from GPS measurements of load-induced deformation. *Geophys Res Lett* 30(14):1742. doi:[10.1029/2003GL017546](https://doi.org/10.1029/2003GL017546)